PHYSICAL REVIEW B **92**, 081108(R) (2015)

Finite-temperature Gutzwiller approximation from the time-dependent variational principle

Nicola Lanatà,* Xiaoyu Deng, and Gabriel Kotliar
Department of Physics and Astronomy, Rutgers University, Piscataway, New Jersey 08856-8019, USA
(Received 8 May 2015; published 11 August 2015)

We develop an extension of the Gutzwiller approximation to finite temperatures based on the Dirac-Frenkel variational principle. Our method does not rely on any entropy inequality, and is substantially more accurate than the approaches proposed in previous works. We apply our theory to the single-band Hubbard model at different fillings, and show that our results compare quantitatively well with dynamical mean field theory in the metallic phase. We discuss potential applications of our technique within the framework of first-principle calculations.

DOI: 10.1103/PhysRevB.92.081108 PACS number(s): 65.40.gd, 71.27.+a

The Gutzwiller approximation (GA) [1–3] is a very useful tool in order to study the ground state of complex strongly correlated electron systems. This important many-body technique has been also formulated and implemented in combination with density functional theory (DFT) [4], e.g., in the LDA+GA approach [5–7], which has been applied successfully to many real materials [7–15]. For strongly correlated metals, the accuracy of the GA is comparable with dynamical mean field theory (DMFT) [16,17], even though the GA is much less computationally demanding. This property makes it an ideal theoretical tool, as numerical speed is essential for the purpose of studying and discovering new materials.

In order to study several temperature-dependent phenomena, such as structural and magnetic transitions and coherence-incoherence crossovers, it would be highly desirable to have at our disposal an extension to finite temperatures of the GA as accurate as the ordinary theory for the ground state. In fact, this would enable us to study these properties also for correlated systems so complex to be out of the reach of the presently available methods, such as DMFT. These motivations have stimulated several previous efforts to generalize the GA to finite temperatures [18–23]. In particular, the extension of the GA derived in Refs. [22,23], which is based on an exact entropy inequality, enables one to evaluate the free energy [23] more accurately than in previous works [18–20]. However, estimating the entropy using an inequality—rather than calculating it exactly—constitutes a source of approximation not present in the GA theory for the ground state, thus leading to finite-temperature results less accurate than at zero temperature.

In this work we introduce an extension of the GA to finite temperatures based on the Dirac-Frenkel variational principle [24–26] and, in particular, on the time-dependent GA theory [27–30] (that we generalize to mixed states). Our method does not rely on any entropy inequality, but only on the variational principle and the Gutzwiller approximation—which are the same approximations done in the ordinary zero-temperature GA. Consequently, as we are going to show, our theory improves considerably the method of Refs. [22,23], and gives results in good quantitative agreement with DMFT for correlated metals, even though it is much less computationally demanding.

*Corresponding author: lanata@physics.rutgers.edu

Imaginary-time evolution. Let us consider a generic system of correlated electrons represented by a Hamiltonian $\hat{\mathcal{H}}$, and define the imaginary-time evolution of a given initial density matrix $\hat{\rho}_0$ as follows:

$$\hat{\rho}(\tau) = e^{-\hat{\mathcal{H}}\tau}\hat{\rho}_0 e^{-\hat{\mathcal{H}}\tau}, \tag{1}$$

i.e., according to the following differential equation:

$$\partial_\tau \hat{\rho}(\tau) = -[\hat{\mathcal{H}}\hat{\rho}(\tau) + \hat{\rho}(\tau)\hat{\mathcal{H}}] \equiv -\{\hat{\mathcal{H}}, \hat{\rho}(\tau)\}. \tag{2}$$

Our aim consists in approximating the imaginary-time dynamics defined above and using it to construct the state of N electrons at temperature T. In fact, if $\tau = \beta/2$ and $\hat{\rho}_0 = \hat{P}_N$ is the projector onto the subspace with N electrons, Eq. (1) reduces to $\hat{P}_N e^{-\beta\hat{\mathcal{H}}}$, which represents a thermal state with $T \equiv 1/\beta$ [31].

In order to derive our approximation scheme, it will be useful to think of $\hat{\rho}$ as the density matrix corresponding to an ensemble of pure states $\{|\Psi_n\rangle\}$,

$$\hat{\rho}(\tau) \equiv \sum_n p_n |\Psi_n(\tau)\rangle\langle\Psi_n(\tau)|, \tag{3}$$

where p_n are fixed probability coefficients. Within this definition, evolving $\hat{\rho}$ according to Eq. (1) amounts to evolving all of the pure states of the ensemble according to the equation

$$d|\Psi_n(\tau)\rangle = -\hat{\mathcal{H}}|\Psi_n(\tau)\rangle d\tau. \tag{4}$$

Note that Eq. (4) resembles a Schrödinger evolution in imaginary time, as it can be obtained from the ordinary real-time Schrödinger evolution

$$d|\Psi_n(t)\rangle = -i\hat{\mathcal{H}}|\Psi_n(t)\rangle dt \tag{5}$$

by substituting $dt \to -i\,d\tau$.

Real-time Dirac-Frenkel scheme. Let us introduce the following action [26]:

$$\mathcal{S}_{\{p_n\}}[\{\Psi_n(t)\}] = \int_{t_i}^{t_f} dt\, \mathcal{L}_{\{p_n\}}[\{\Psi_n(t)\}], \tag{6}$$

$$\mathcal{L}_{\{p_n\}}[\{\Psi_n\}] \equiv \sum_n p_n \langle\Psi_n|\, i\partial_t - \hat{\mathcal{H}}\,|\Psi_n\rangle = \sum_n p_n \langle\Psi_n|\, i\partial_t\,|\Psi_n\rangle - \mathcal{E}, \tag{7}$$

where $\mathcal{E} \equiv \sum_n p_n \langle\Psi_n|\,\hat{\mathcal{H}}\,|\Psi_n\rangle$. Note that $\mathcal{S}_{\{p_n\}}$ depends parametrically on the probability coefficients p_n, which are fixed

and depend only on the initial condition. From now on we refer to Eq. (6) as the Dirac-Frenkel action.

It can be readily verified that, regardless of the values of p_n, the exact solution of the Lagrange equations for the ensemble of states $\{|\Psi_n(t)\rangle\}$ is given by Eq. (5).

The key advantage of the Dirac-Frenkel characterization of the time evolution outlined above is that it allows us to build up a well-founded variational approximation scheme for the time evolution [Eq. (5)] as follows.

Let us assume that we want to solve approximately the time-dependent problem by restricting the search of the solution within a subset $\mathcal{M}$ of trial ensembles $\{|\Psi_n\rangle\}$. Once we are able to evaluate the action S along any given trajectory in $\mathcal{M}$, the Dirac-Frenkel variational principle provides us with a prescription to approximate the instantaneous time evolution of any $\{|\Psi_n\rangle\} \in \mathcal{M}$. Note that, by construction, this time evolution is such that $\{|\Psi_n(t)\rangle\} \in \mathcal{M}\ \forall t$.

Application to the GA. For the sake of simplicity, in this work the method will be formulated for the single-band Hubbard model:

$$\hat{\mathcal{H}} = \sum_{R\neq R'}\sum_{\sigma=\uparrow,\downarrow} \epsilon_{RR'}\, c^{\dagger}_{R\sigma} c_{R'\sigma} + U \sum_{R} c^{\dagger}_{R\uparrow} c_{R\uparrow} c^{\dagger}_{R\downarrow} c_{R\downarrow}, \quad (8)$$

where R is the site label and σ is the spin label. This model will be studied at generic filling $N/\mathcal{N} = 1+\delta$, where $\mathcal{N}$ is the number of sites and δ is the doping. Furthermore, a paramagnetic solution will be assumed. The extension to multiband Hubbard models is straightforward, and its numerical implementation will be discussed in a future work.

Here we want to search for the saddle point of the Dirac-Frenkel action within the set $\mathcal{M}_G$ of ensembles of Gutzwiller states represented as follows:

$$\{|\Psi_n\rangle\} = \{\hat{\mathcal{P}}_G\,|\Psi_{0n}\rangle\} \equiv \mathcal{M}_G, \quad (9)$$

where $|\Psi_{0n}\rangle$ are Slater determinants and $\hat{\mathcal{P}}_G \equiv \prod_R \hat{\mathcal{P}}_R$ is an operator whose local components are defined as $\hat{\mathcal{P}}_R \equiv \sum_{\Gamma\Gamma'} \Lambda_{\Gamma\Gamma'}\,|R,\Gamma\rangle\langle R',\Gamma|$, where $\Lambda_{\Gamma\Gamma'}$ are generally complex numbers and $|R,\Gamma\rangle\langle R,\Gamma'|$ act onto the corresponding local many-body states $|R,\Gamma\rangle \in \{|0\rangle, |R,\uparrow\rangle, |R,\downarrow\rangle, |R,\uparrow\downarrow\rangle\}$. Note that from the assumptions that $\hat{\mathcal{P}}_R$ conserves the number of electrons and is spin rotationally invariant it follows that the off-diagonal elements of Λ are zero.

The physical density matrix corresponding to the ensemble [Eq. (9)] is

$$\hat{\rho}_G \equiv \hat{\mathcal{P}}_G \hat{\rho}_0^{*} \hat{\mathcal{P}}_G^{\dagger}, \quad (10)$$

where

$$\hat{\rho}_0^{*} \equiv \sum_n p_n |\Psi_{0n}\rangle\langle\Psi_{0n}| \Big/ \sum_n p_n \langle\Psi_{0n}|\Psi_{0n}\rangle \quad (11)$$

is called variational density matrix. We assume that $\hat{\rho}_0^{*}$ can be represented as the Boltzmann distribution of a generic noninteracting Hamiltonian $\forall t$.

Note that the variational form of $\hat{\rho}_G$ is exactly the same as in Ref. [23]. Consequently, the same procedure can be applied to evaluate the total energy corresponding to $\hat{\rho}_G$, which is necessary to evaluate the Dirac-Frenkel action [see Eq. (7)]. Let us summarize the main steps of this procedure. (1) The set of ensembles $\mathcal{M}_G$ is restricted by the so-called Gutzwiller constraints [22,23,32]:

$$\mathrm{Tr}[\hat{\rho}_0^{*} \hat{\mathcal{P}}_R^{\dagger} \hat{\mathcal{P}}_R] = 1, \quad (12)$$

$$\mathrm{Tr}[\hat{\rho}_0^{*} \hat{\mathcal{P}}_R^{\dagger} \hat{\mathcal{P}}_R\, c^{\dagger}_{R\sigma} c_{R\sigma}] = \mathrm{Tr}[\hat{\rho}_0^{*} c^{\dagger}_{R\sigma} c_{R\sigma}] = [1+\delta]/2. \quad (13)$$

(2) The Gutzwiller approximation is assumed [3], which is an approximation scheme that, as DMFT [16], becomes exact in the limit of infinite coordination lattices. As in Ref. [23], we introduce the matrix of slave-boson amplitudes:

$$\phi_{\Gamma\Gamma'} = \delta_{\Gamma\Gamma'} \Lambda_{\Gamma\Gamma} \sqrt{P^0_{\Gamma}}, \quad (14)$$

$$P^0_{\Gamma} \equiv \mathrm{Tr}[\hat{\rho}_0^{*} |R,\Gamma\rangle\langle R,\Gamma|]. \quad (15)$$

(3) Within the above definitions and the Gutzwiller approximation, the Gutzwiller constraints can be represented as

$$\mathrm{Tr}[\phi^{\dagger}\phi] = 1, \quad (16)$$

$$\mathrm{Tr}[\phi^{\dagger}\phi F^{\dagger}_{\sigma} F_{\sigma}] = \mathrm{Tr}[\hat{\rho}_0^{*} c^{\dagger}_{R\sigma} c_{R\sigma}] = [1+\delta]/2, \quad (17)$$

where $[F_{\sigma}]_{\Gamma\Gamma'} \equiv \langle\Gamma\,|c_{R\sigma}|\,\Gamma'\rangle$. (4) Furthermore, it can be shown that $\phi\phi^{\dagger}$ represents the local reduced density matrix in the basis $\{|R,\Gamma\rangle\}$, while the expectation values of the intersite single-particle density-matrix operators is given by

$$\mathrm{Tr}[\hat{\rho}_G c^{\dagger}_{R\sigma} c_{R'\sigma}] = |\mathcal{R}|^2 \mathrm{Tr}[\hat{\rho}_0^{*} c^{\dagger}_{R\sigma} c_{R'\sigma}] \qquad \forall R \neq R', \quad (18)$$

where $\mathcal{R} = \mathrm{Tr}[\phi^{\dagger} F^{\dagger}_{\sigma} \phi F_{\sigma}]/[1-\delta^2]^{1/2}$.

The above equations enable us to evaluate the total energy $\mathcal{E}$ [23], which enters in the definition of the GA Dirac-Frenkel Lagrange function [see Eq. (7)]. The term of Eq. (7) involving the time derivative can be readily evaluated following Ref. [29]. In conclusion, thanks to the equations above, the GA Dirac-Frenkel Lagrange function can be rewritten as follows:

$$\begin{aligned}
&\mathcal{L}_{\{p_n\}}[\{\Psi_{0n}\};\phi,\mathcal{R},\mathcal{R}^{*},\mathcal{D},\mathcal{D}^{*}] \\
&\quad = \sum_n p_n \langle\Psi_{0n}|\, i\partial_t - |\mathcal{R}|^2 \sum_{R\neq R'}\sum_{\sigma=\uparrow,\downarrow} \epsilon_{RR'} c^{\dagger}_{R\sigma} c_{R'\sigma}\,|\Psi_{0n}\rangle \\
&\qquad + \mathcal{N}\,\mathrm{Tr}[\phi^{\dagger} i\partial_t \phi] - \mathcal{N}\,\mathrm{Tr}[U\phi\phi^{\dagger} F^{\dagger}_{\uparrow} F_{\uparrow} F^{\dagger}_{\downarrow} F_{\downarrow}] \\
&\qquad - \mathcal{N} \sum_{\sigma=\uparrow,\downarrow} (\mathrm{Tr}[\mathcal{D}\phi^{\dagger} F^{\dagger}_{\sigma} \phi F_{\sigma}] - \mathcal{D}\mathcal{R}[1-\delta^2]^{1/2} + \mathrm{c.c.}).
\end{aligned} \quad (19)$$

Note that, following Ref. [7], we have formally enforced the definition of $\mathcal{R}$ using the Lagrange multiplier $\mathcal{D}$.

The Lagrange equations for the real-time dynamics induced by Eq. (19) are the following:

$$\left[i\partial_t - \hat{\mathcal{H}}^{\mathrm{Re}}_{\mathrm{qp}}[\mathcal{R},\mathcal{R}^{*}]\right]|\Psi_{0n}\rangle = 0 \quad \forall n, \quad (20)$$

$$\left[i\partial_t - H^{\mathrm{Re}}_{\mathrm{emb}}[\mathcal{D},\mathcal{D}^{*}]\right]\phi = 0, \quad (21)$$

$$\mathcal{R} = \mathrm{Tr}[\phi^{\dagger} F^{\dagger}_{\sigma} \phi F_{\sigma}][1-\delta^2]^{-1/2}, \quad (22)$$

$$\mathcal{D} = 2[1-\delta^2]^{-1/2} \mathrm{Tr}\left[\hat{\rho}_0^{*} \frac{\partial}{\partial\mathcal{R}} \hat{\mathcal{H}}^{\mathrm{Re}}_{\mathrm{qp}}[\mathcal{R},\mathcal{R}^{*}]\right], \quad (23)$$

where

$$\hat{\mathcal{H}}^{\mathrm{Re}}_{\mathrm{qp}}[\mathcal{R},\mathcal{R}^*] \equiv |\mathcal{R}|^2 \sum_{R\neq R'} \sum_{\sigma} \epsilon_{RR'} c^{\dagger}_{R\sigma} c_{R'\sigma}, \tag{24}$$

$$H^{\mathrm{Re}}_{\mathrm{emb}}[\mathcal{D},\mathcal{D}^*]\phi \equiv \frac{\delta}{\delta\phi^{\dagger}} \Big\{ \mathrm{Tr}[U\,\phi\phi^{\dagger}\, F^{\dagger}_{\uparrow} F_{\uparrow} F^{\dagger}_{\downarrow} F_{\downarrow}] + \sum_{\sigma} (\mathrm{Tr}[\mathcal{D}\,\phi^{\dagger} F^{\dagger}_{\sigma} \phi F_{\sigma}] + \mathrm{c.c.}) \Big\} \phi. \tag{25}$$

Note that the generator of the instantaneous evolution is quadratic and identical for all of the $|\Psi_{0n}\rangle$, and that also the evolution of ϕ resembles formally a time-dependent Schrödinger equation.

The instantaneous real-time evolution described by the equations above corresponds to applying well-defined increments on all of the states of $\mathcal{M}_G$ [see Eq. (9)]. We may represent these increments as follows:

$$d|\Psi_n\rangle = [(\partial_t \hat{\mathcal{P}}_G)|\Psi_{0n}\rangle + \hat{\mathcal{P}}_G(\partial_t|\Psi_{0n}\rangle)]dt. \tag{26}$$

Imaginary-time dynamics. Our goal consists in modifying the real-time GA dynamics defined above in order to approximate the imaginary-time evolution [Eq. (4)].

The formal similarity between Eqs. (4) and (5) suggests that it is possible to approximate the imaginary-time evolution of $\{|\Psi_n\rangle\}$ simply by substituting $dt \to -i\,d\tau$ in Eq. (26). It can be readily verified that this prescription would amount to updating the Gutzwiller variational parameters [see Eqs. (14) and (15)] as follows [33]:

$$\big[\partial_\tau + \hat{\mathcal{H}}^{\mathrm{Re}}_{\mathrm{qp}}[\mathcal{R},\mathcal{R}^*]\big]|\Psi_{0n}\rangle = 0 \quad \forall n, \tag{27}$$

$$\big[\partial_\tau + H^{\mathrm{Re}}_{\mathrm{emb}}[\mathcal{D},\mathcal{D}^*]\big]\phi = 0. \tag{28}$$

Unfortunately, Eqs. (27) and (28) violate the Gutzwiller constraints [see Eqs. (16) and (17)]. Consequently, similarly to Ref. [34], it is necessary to define a "projection scheme" in order to enforce them at every time step.

Here we propose to enforce Eqs. (16) and (17) by using the following prescription:

$$\big[\partial_\tau + \hat{\mathcal{H}}^{\mathrm{Im}}_{\mathrm{qp}}[\mathcal{R},\mathcal{R}^*,E_0]\big]|\Psi_{0n}\rangle = 0 \quad \forall n, \tag{29}$$

$$\big[\partial_\tau + H^{\mathrm{Im}}_{\mathrm{emb}}[\mathcal{D},\mathcal{D}^*,\lambda^c,E^c]\big]\phi = 0, \tag{30}$$

where the "generators" have been modified as follows:

$$\hat{\mathcal{H}}^{\Im}_{\mathrm{qp}} \equiv \hat{\mathcal{H}}^{\mathrm{Re}}_{\mathrm{qp}} - E_0, \tag{31}$$

$$H^{\mathrm{Im}}_{\mathrm{emb}}\phi \equiv H^{\mathrm{Re}}_{\mathrm{emb}}\phi + \frac{\delta\,\mathrm{Tr}\big[\lambda^c \sum_\sigma \phi^{\dagger}\phi F^{\dagger}_{\sigma} F_{\sigma} - E^c \phi^{\dagger}\phi\big]}{\delta\phi^{\dagger}}\phi, \tag{32}$$

and $E_0(\tau)$ is constructed in order to enforce the normalization condition of $\hat{\rho}^*_0$ [see Eq. (11)], while $E^c(\tau)$ and $\lambda^c(\tau)$ are constructed in order to enforce Eqs (16) and (17), respectively.

We point out that the procedure defined above enables us to recover the ordinary GA theory for the ground state at $\tau \to \infty$. In fact, within the formulation of Ref. [7], the GA parameters of the ground state are obtained as the ground states of $\hat{\mathcal{H}}^{\mathrm{Im}}_{\mathrm{qp}}$ and $H^{\mathrm{Im}}_{\mathrm{emb}}$, which correspond to a fixed point of our imaginary-time dynamics.

It can be readily verified that Eq. (29) implies that the imaginary-time evolution of the variational density matrix is given by

$$\hat{\rho}^*_0(\tau) = \hat{P}_N e^{-2\int_0^\tau d\tau' [Z(\tau')\sum_{R\neq R',\sigma} \epsilon_{RR'} c^{\dagger}_{R\sigma} c_{R'\sigma} - E_0(\tau')]}, \tag{33}$$

where $Z(\tau') \equiv |\mathcal{R}(\tau')|^2$ is the Gutzwiller quasiparticle weight, and $E_0(\tau')$ is constructed in order to enforce the normalization condition of $\hat{\rho}^*_0(\tau)$ for all imaginary times. In fact, Eq. (33) satisfies

$$\partial_\tau \hat{\rho}^*_0(\tau) = -\big\{H^{\mathrm{Im}}_{\mathrm{qp}}(\tau), \hat{\rho}^*_0(\tau)\big\}, \tag{34}$$

which is consistent with Eq. (29), and enables us to avoid keeping track of the time evolution of all of the states of $\mathcal{M}_G$ (which would be practically impossible).

Note that, since we are in the thermodynamical limit, the expectation values with respect to $\hat{\rho}^*_0(\tau)$ can be evaluated in the grand-canonical ensemble, i.e., we can assume that

$$\hat{\rho}^*_0(\tau) \propto e^{-\beta^*_0(\tau)[\sum_{R\neq R',\sigma} \epsilon_{RR'} c^{\dagger}_{R\sigma} c_{R'\sigma} - \mu^*_0(\tau)\hat{N}]}, \tag{35}$$

where $\beta^*_0(\tau) \equiv 2\int_0^\tau d\tau' Z(\tau')$, $\hat{N}$ is the number operator, and $\mu^*_0(\tau)$ is such that the system has N electrons on average.

The imaginary-time evolution of the slave-boson amplitudes is obtained by substituting Eq. (35) into the other Lagrange equations and solving them numerically. A possible numerical implementation is explained in detail in the Supplemental Material [35].

Numerical results. Let us now discuss our numerical calculations of the Hubbard model [see Eq. (8)]. We assume a semicircular density of states (corresponding to a Bethe lattice in infinite dimensions) [36] and set the half-bandwidth D as the unit of energy. For comparison, we perform DMFT calculations using the continuous time quantum Monte Carlo method [37,38] as impurity solver, as implemented in TRIQS [39].

Note that in the following calculations the entropy will not be calculated directly from the GA variational parameters (which could be done only approximately [23]), but will be evaluated as a by-product of the imaginary-time evolution of the total energy, i.e., by using the thermodynamical identity $dS = d\mathcal{E}/T$ and fixing the constant of integration in such a way that at $S(T=\infty)$ is exact.

In Fig. 1 is shown the evolution of the double occupancy $d \equiv \langle c^{\dagger}_{R\uparrow} c_{R\uparrow} c^{\dagger}_{R\downarrow} c_{R\downarrow}\rangle$ (upper panel) and the total energy (lower panel) as a function of the temperature at half-filling for several values of U. In the inset is shown the corresponding entropy for $U/D = 1.95$. The GA results are shown in comparison with DMFT and the Gutzwiller data of Ref. [22].

The agreement between the GA and DMFT+CTQMC is quantitatively satisfactory, especially for smaller values of U and higher temperatures (i.e., when the system is less correlated). Indeed, our method substantially improves the results obtained within the approximation scheme of Ref. [22]. The slight quantitative discrepancy with DMFT for larger U's reflects the known fact that the Mott insulator is not well described by the GA, but is approximated by the simple atomic limit, which is a state with $d = 0$. However, as long as the system is metallic, our extension of the GA to finite

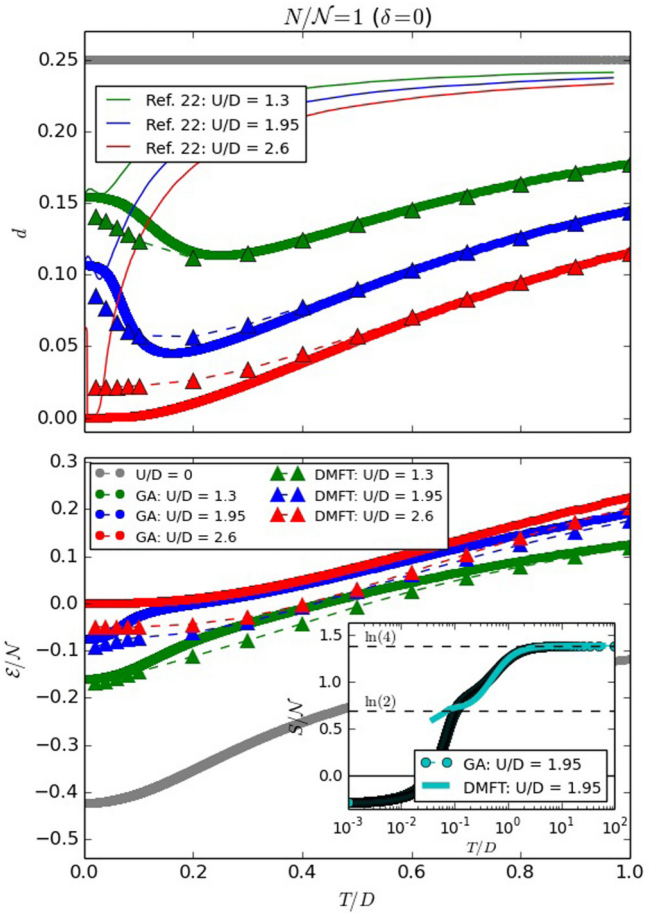

FIG. 1. (Color online) GA calculations of the single-band Hubbard model at half-filling ($N/\mathcal{N} = 1$) in comparison with DMFT+CTQMC and the data of Ref. [22]. Upper panel: Temperature dependence of the double occupancy. Lower panel: Temperature dependence of total energy per site. Inset of the lower panel: Temperature dependence of the GA entropy per site in comparison with DMFT.

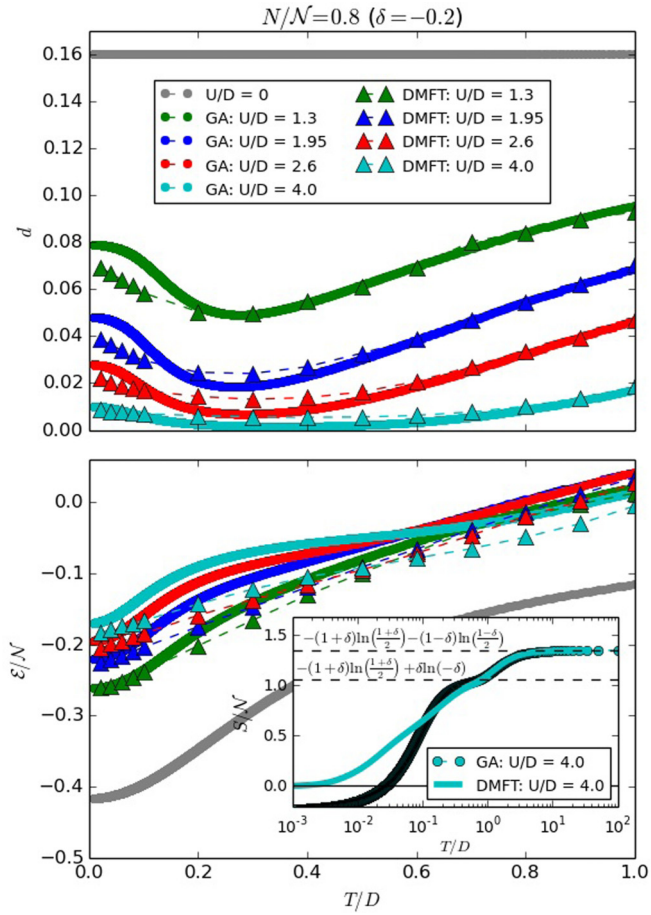

FIG. 2. (Color online) GA calculations of the single-band Hubbard model away from half-filling ($N/\mathcal{N} = 0.8$) in comparison with DMFT+CTQMC. Upper panel: Temperature dependence of the double occupancy. Lower panel: Temperature dependence of the total energy per site. Inset of the lower panel: Temperature dependence of the GA entropy per site in comparison with the DMFT data of Ref. [40].

temperatures is remarkably accurate. Also the GA entropy is in reasonable agreement with DMFT and, in particular, it displays the expected plateau at $S \simeq \ln(2)$ [40]. However, since the integral of dS over the whole range of temperatures is not exact, the GA entropy does not vanish at $T \to 0$, even though, as pointed out before, the GA solution is actually a pure state in this limit. Note that DMFT does not suffer this inconvenience because it is an exact theory in infinite dimensions, while the GA is a variational approximation in this limit.

Let us now consider the Hubbard model away from half-filling. In particular, we consider the case of $N/\mathcal{N} = 0.8$ electrons per site (i.e., $\delta = -0.2$). In the upper panel of Fig. 2 is shown the temperature dependence of the double occupancy for several values of U, while in the lower panel is shown the evolution of the total energy $\mathcal{E}$. Finally, in the inset of the lower panel is shown the temperature dependence of the entropy for $U/D = 4$, in comparison with the DMFT entropy calculated in Ref. [40].

The agreement between the GA and DMFT+CTQMC is even better for $N/\mathcal{N} = 0.8$ than for half-filling (which is to be expected, as the doped system is metallic for all U's). It is especially remarkable the fact that the behavior of S is satisfactory for $U/D = 4$, which is the largest interaction strength considered. In particular, we point out that the position of the plateau is in excellent agreement with DMFT, and is consistent with the expected value based on the atomic limit: $S \simeq -(1+\delta)\ln(\frac{1+\delta}{2}) + \delta\ln(-\delta)$. Note that for the doped system the value of S at $T \to \infty$ is $-(1+\delta)\ln(\frac{1+\delta}{2}) - (1-\delta)\ln(\frac{1-\delta}{2})$], which is slightly smaller than ln(4).

In conclusion, using the Dirac-Frenkel variational principle, we have developed an extension of the GA to finite temperatures as accurate as the ordinary GA theory for the ground state. We have performed benchmark calculations of the single-band Hubbard model at different fillings, and compared our results with DMFT+CTQMC, finding good quantitative agreement between the two methods in the metallic phase. We believe that our method will enable us to calculate from first principles several important physical quantities—such as the specific heat, the entropy, and the temperature-dependent structural properties—of strongly correlated systems presently too complex to be studied with more accurate methods,

such as DMFT. It will also be interesting to see whether the imaginary-time scheme proposed in this work can be used to develop an efficient numerical alternative strategy to calculate the GA ground state of complex multiband systems.

Acknowledgments. We thank Michele Fabrizio for useful discussions, Michel Ferrero for providing us with his DMFT code, and Qiang-Hua Wang for allowing us to use his data in Fig. 1. This work was supported by US DOE Office of Basic Energy Sciences under Grant No. DE-FG02-99ER45761.

[1] M. C. Gutzwiller, Phys. Rev. Lett. **10**, 159 (1963).
[2] M. C. Gutzwiller, Phys. Rev. **134**, A923 (1964).
[3] M. C. Gutzwiller, Phys. Rev. **137**, A1726 (1965).
[4] P. Hohenberg and W. Kohn, Phys. Rev. **136**, B864 (1964).
[5] X.-Y. Deng, L. Wang, X. Dai, and Z. Fang, Phys. Rev. B **79**, 075114 (2009).
[6] K. M. Ho, J. Schmalian, and C. Z. Wang, Phys. Rev. B **77**, 073101 (2008).
[7] N. Lanatà, Y. X. Yao, C.-Z. Wang, K.-M. Ho, and G. Kotliar, Phys. Rev. X **5**, 011008 (2015).
[8] F. Lu, J.-Z. Zhao, H. Weng, Z. Fang, and X. Dai, Phys. Rev. Lett. **110**, 096401 (2013).
[9] G.-T. Wang, Y. Qian, G. Xu, X. Dai, and Z. Fang, Phys. Rev. Lett. **104**, 047002 (2010).
[10] T. Schickling, F. Gebhard, J. Bünemann, L. Boeri, O. K. Andersen, and W. Weber, Phys. Rev. Lett. **108**, 036406 (2012).
[11] S. Zhou and Z. Q. Wang, Phys. Rev. Lett. **105**, 096401 (2010).
[12] J.-P. Julien and J. Bouchet, in *Recent Advances in the Theory of Chemical and Physical Systems*, edited by J.-P. Julien, J. Maruani, D. Mayou, S. Wilson, and G. Delgrado-Barrio, Progress in Theoretical Chemistry and Physics Vol. 15 (Springer, Netherlands, 2006), p. 509.
[13] N. Lanatà, H. U. R. Strand, G. Giovannetti, B. Hellsing, L. de'Medici, and M. Capone, Phys. Rev. B **87**, 045122 (2013).
[14] N. Lanatà, Y. X. Yao, C. Z. Wang, K. M. Ho, J. Schmalian, K. Haule, and G. Kotliar, Phys. Rev. Lett. **111**, 196801 (2013).
[15] N. Lanatà, Y. X. Yao, C.-Z. Wang, K.-M. Ho, and G. Kotliar, Phys. Rev. B **90**, 161104 (2014).
[16] A. Georges, G. Kotliar, W. Krauth, and M. J. Rozenberg, Rev. Mod. Phys. **68**, 13 (1996).
[17] V. Anisimov and Y. Izyumov, *Electronic Structure of Strongly Correlated Materials* (Springer, New York, 2010).
[18] K. A. Chao and K. F. Berggren, Phys. Rev. B **15**, 1656 (1977).
[19] T. M. Rice, K. Ueda, H. R. Ott, and H. Rudigier, Phys. Rev. B **31**, 594 (1985).
[20] G. Kotliar and A. E. Ruckenstein, Phys. Rev. Lett. **57**, 1362 (1986).
[21] H. Hasegawa, J. Phys.: Condens. Matter **1**, 9325 (1989).
[22] W.-S. Wang, X.-M. He, D. Wang, Q.-H. Wang, Z. D. Wang, and F. C. Zhang, Phys. Rev. B **82**, 125105 (2010).
[23] M. Sandri, M. Capone, and M. Fabrizio, Phys. Rev. B **87**, 205108 (2013).
[24] P. A. M. Dirac, Proc. Cambridge Philos. Soc. **26**, 376 (1930).
[25] J. Frenkel, *Wave Mechanics: Advanced General Theory* (Clarendon, Oxford, 1934).
[26] A. R. DeAngelis and G. Gatoff, Phys. Rev. C **43**, 2747 (1991).
[27] G. Seibold and J. Lorenzana, Phys. Rev. Lett. **86**, 2605 (2001).
[28] M. Schirò and M. Fabrizio, Phys. Rev. Lett. **105**, 076401 (2010).
[29] M. Fabrizio, in *New Materials for Thermoelectric Applications: Theory and Experiment*, NATO Science for Peace and Security Series B: Physics and Biophysics, edited by V. Zlatic and A. Hewson (Springer, Netherlands, 2013), pp. 247–273.
[30] N. Lanatà and H. U. R. Strand, Phys. Rev. B **86**, 115310 (2012).
[31] M. Zwolak and G. Vidal, Phys. Rev. Lett. **93**, 207205 (2004).
[32] M. Fabrizio, Phys. Rev. B **76**, 165110 (2007).
[33] Note that for this system P^0 is constant, as it depends only on the doping δ, which is fixed.
[34] J. Haegeman, J. I. Cirac, T. J. Osborne, I. Pižorn, H. Verschelde, and F. Verstraete, Phys. Rev. Lett. **107**, 070601 (2011).
[35] See Supplemental Material at http://link.aps.org/supplemental/10.1103/PhysRevB.92.081108 for details about the numerical implementation.
[36] Note that DMFT is an exact theory for this system.
[37] A. N. Rubtsov, V. V. Savkin, and A. I. Lichtenstein, Phys. Rev. B **72**, 035122 (2005).
[38] P. Werner, A. Comanac, L. de'Medici, M. Troyer, and A. J. Millis, Phys. Rev. Lett. **97**, 076405 (2006).
[39] O. Parcollet, M. Ferrero, T. Ayral, H. Hafermann, I. Krivenko, L. Messio, and P. Seth, Comput. Phys. Commun. (2015).
[40] X. Deng, J. Mravlje, R. Žitko, M. Ferrero, G. Kotliar, and A. Georges, Phys. Rev. Lett. **110**, 086401 (2013).